The effect of a continuous NiO heterolayer on leakage Currents in β-Ga_2O_3-based schottky barrier diodes

© N.N. Yakovlev[1], B.O. Kushnarev[1], A.V. Almaev[2], A.V. Tsymbalov[1], V.V. Kopyev[1], D.A. Almaev[1]

[1] Research and Development Center Advanced Technologies in Microelectronics, National Research Tomsk State University, 634050 Tomsk, Russia
[2] Department of Semiconductor Electronics, Faculty of Radiophysics, National Research Tomsk State University, 634050 Tomsk, Russia

E-mail: nik_mr_x@mail.ru

Received May 23, 2026
Revised August 4, 2026
Accepted August 11, 2026

The influence of a continuous NiO heterolayer on leakage currents and electrophysical characteristics of Schottky barrier diodes based on β-Ga_2O_3 was investigated.

The NiO film was deposited by high-frequency magnetron sputtering and is polycrystalline with a crystallite size of ~ 31.6 nm. The fabricated Schottky diodes exhibited a high rectification ratio of $5.44 \cdot 10^7$ and a breakdown voltage of 171 V, corresponding to an electric field strength of 3.55 MV/cm. The introduction of the NiO heterolayer reduced the reverse leakage current density by 2–3 orders of magnitude due to the formation of a heterojunction barrier and partial suppression of the edge effect. A comprehensive analysis of the reverse I–V characteristics revealed a sequential change in the leakage current mechanisms from thermionic field emission at $|U| \leq 45$ V to space-charge-limited current at $|U| > 115$ V.

Keywords: gallium oxide, Schottky barrier diode, leakage currents, power electronics.

DOI: 10.61011/SC.2026.04.64081.9913

1. Introduction

Gallium oxide (β-Ga_2O_3) is related to ultrawide-bandgap semiconductors and is actively studied as one of the most promising materials for power electronics of the next generation [1–5]. The development of Schottky barrier diodes (SBD) based on β-Ga_2O_3 is of the greatest interest, which are key components of the energy conversion systems for electric vehicles, power conditioning and distribution systems [6–15]. Due to a wide band gap ($E_g \approx 4.8$–4.9 eV), high intensity of electric breakdown field ($E_b \approx 8.2$ MV/cm) and high value of Baliga figure-of-merit (BFOM) β-Ga_2O_3 significantly exceeds SiC and GaN as the material for power electronics [9–13]. The ability to grow by most available bulk crystal growth methods (Czochralski methods, zone melting etc.) is the advantage, making it possible to obtain wafers of larger diameter (4–6 inches), which provides for high structural quality and low cost of manufacture compared to SiC and GaN [14,15].

However, today in SBDs based on β-Ga_2O_3 significant problems are observed: high reverse leakage current density, early breakdown at the edge of the structure due to localization of the electric field (edge effect), which prevents achievement of the theoretically possible value of breakdown voltage (3–8 kV) [1,16].

One of the most promising approaches to improve the breakdown voltage is the use of a heterogeneous transition in virtue of absence of Ga_2O_3 p-type of conductivity. The following are used most often as semiconductors for heterojunctions with β-Ga_2O_3: NiO, Cu_2O, GaN, SnO [17–20]. Among them NiO has some advantages: wide band gap (3.6–4.0 eV), high structural compatibility (mismatch of NiO (111) and β-Ga_2O_3 ($\bar{2}01$) lattices is only 0.46 %) [17–20], easily forms a p–n-like heterojunction from Ga_2O_3 and makes it possible to effectively decrease the peak field at the edge of the anode [17]. The key advantage is the ability to deposit the NiO layers by the method of magnetron sputtering. This method provides for good reproducibility, control of stoichiometry (at the expense of the ratio of Ar/O_2) and low cost [21].

The literature previously demonstrated high voltage SBDs on β-Ga_2O_3 with a NiO heterolayer obtained by magnetron sputtering [1,16,22,23]. Thus, the papers show achievement of breakdown voltage $U_b \geq 3$ kV using multi-layer gradient NiO layers, and also the considerable decrease in the capacitance and improvement of dynamic characteristics [1,22].

This paper is dedicated to the development and study of vertical diodes with Schottky barrier based on β-Ga_2O_3 with a NiO heterolayer formed by the method of magnetron sputtering. Primary attention is paid to the effect of the solid heterogeneous NiO layer on the mechanisms of reverse leakage current and electric characteristics of SBDs.

2. Method

Substrates in manufacture of SBDs were commercial unintentionally doped substrates β-Ga_2O_3 with orientation

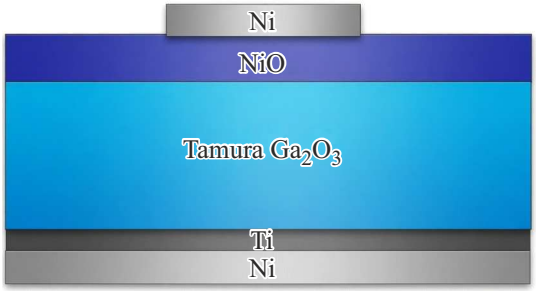


Figure 1. Schematic image of SBD based on β-Ga_2O_3 with the NiO layer.

($\bar{2}01$) (Tamura corp., Japan). The thickness of substrates was 650 μm, and the concentration of impurity $N_d \sim 10^{17}$ cm^{-3}.

A solid NiO layer with thickness of $\sim$ 200 nm was formed on the surface of the substrates using magnetron sputtering from a metal Ni-target in Ar/O_2-plasma in an Edwards A-500 (UK) setup. The concentration of oxygen in the gas mixture was maintained as 56.0 ± 0.5 %. After sputtering of the layer, the structures were annealed for 60 min and at temperature of 800 °C in the air atmosphere.

After that onto surfaces β-Ga_2O_3 using vacuum thermal evaporation, solid Ti layers with thickness of 20 nm and Ni layers with thickness of 100 nm were applied at pressure of $\sim 10^{-4}$ Pa. After thermal evaporation of the Ti/Ni layers the structure was subjected to fast thermal annealing at temperature of 400 °C in vacuum for 1 min. On the NiO surface a Ni-anode was formed with diameter of 1 mm and thickness of 100 nm via a shadow mask (Figure 1).

To determine the phase composition of structure NiO/β-Ga_2O_3, X-ray diffraction method (XRD) was used. Measurements with XRD method were conducted on an X'PERT PRO diffractometer with radiation of CuK_α at voltage of 40 kV and current of 30 mA, in goniometric mode ($\theta - 2\theta$). Measurements were carried out from the side of the substrate β-Ga_2O_3 and from the side of the NiO layer.

The spectra of optical transmission in the wavelength range λ from 250 to 570 nm were measured with a spectrometer Ocean Optics with resolution of 1 nm. The source of radiation was a deuterium lamp D-2000 Micropack.

Current voltage (I–V) and capacitance voltage (C–V) curves were measured using a Keithley 2636A source-measure unit and an RLC-meter Agilent E4980A, accordingly. Measurements of electrophysical characteristics were carried out in dark conditions in a measurement chamber Nextron MPS-CHH, equipped with microprobes of clamped type.

3. Study of structural properties

XRD spectrum of NiO/β-Ga_2O_3 structure is shown in Figure 2. The found high-intensity peaks β-Ga_2O_3 are associated with reflections from planes ($\bar{2}01$), ($\bar{4}02$), ($\bar{6}03$) and ($\bar{8}04$) β-Ga_2O_3 (ICSD#83645). Peaks at $2\theta = 37.4$ and 79.5° correspond to the reflections from the planes (111) and (222) for NiO (JCPDS No. 47-1049). It should be noted that orientation (111) is dominant, when grown on β-Ga_2O_3 other NiO peaks were not observed [17–19]. The NiO (111) peak has a full width at half maximum (FWHM) at 0.27°). The film is polycrystalline and highly textured (most crystallites have their (111) planes parallel to the substrate β-Ga_2O_3. The size of crystallites is $\sim$ 31.6 nm.

Transmission spectra of NiO/β-Ga_2O_3 structures are shown in Figure 3. Values of the transmittance for NiO/β-Ga_2O_3 structures in the interval of $\lambda = 400-560$ nm exceed 70 %. The range of short wavelengths shows a dramatic decrease in the transmittance, which is due to interband absorption. The analysis of the edge of absorption in the structures showed that the optical width of the band

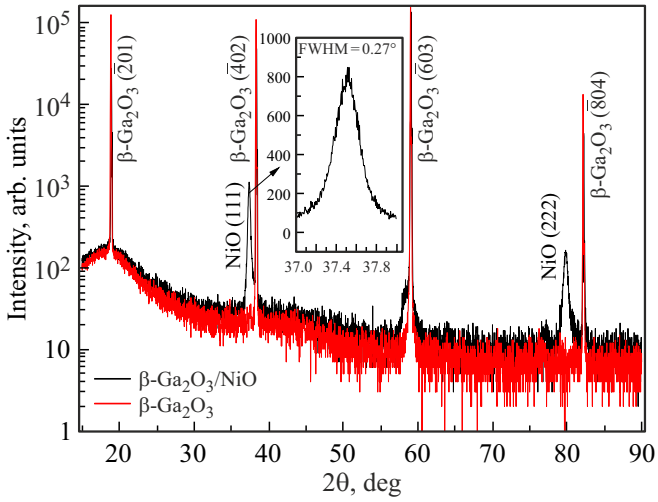


Figure 2. XRD spectra of NiO/β-Ga_2O_3 structure obtained from the side of β-Ga_2O_3 substrate (red) and from the side of NiO layer (black).

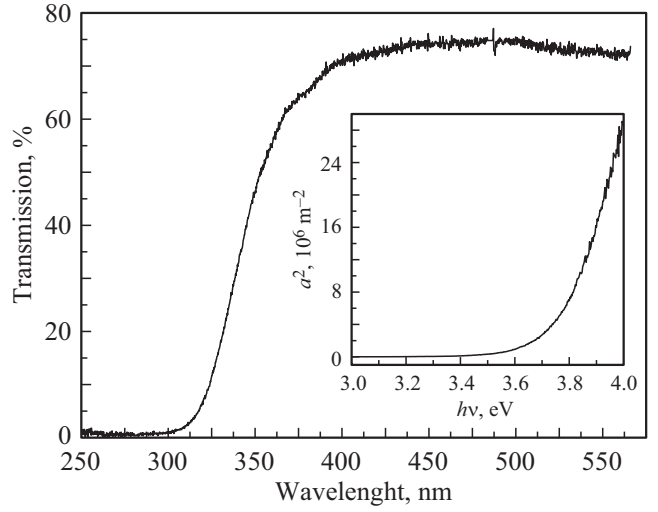


Figure 3. Optical transmission spectrum of NiO/β-Ga_2O_3 structure.

gap E_g^{op} is 3.7 ± 0.1 eV (see insert to Figure 3), which corresponds to NiO [18,19].

4. Study of electrophysical characteristics of SBD

Figure 4 presents capacitance voltage curves of Schottky diodes obtained at amplitude of alternating signal of 100 mV and its frequency of 1 kHz. Based on C–V curve analysis in coordinates S^2/C^2 from U the effective concentration of $N_d - N_a = 2.3 \cdot 10^{17}$ cm^{-3} in the gallium oxide substrate was determined using the formula

$$N_d - N_a = \frac{2}{e\varepsilon_r\varepsilon_0 B}, \quad (1)$$

where e is charge of electron; $\varepsilon_r = 10$ is dielectric permittivity for β-Ga_2O_3; B is inclination of reverse branch of C–V curve in coordinates S^2/C^2 from U (see insert to Figure 4). The value of the contact potential difference U_k was determined by linear extrapolation of dependence S^2/C^2 on the applied voltage until crossing with the abscissa axis and was 1.29 V.

Experimental dependences of the current density on the applied voltage of Schottky diodes at room temperature are shown in Figure 5. I–V curves were measured in the voltage range from −10 to 5 V. The SBD rectification ratio at ±2 V was $5.44 \cdot 10^7$.

Based on the obtained data, the I–V curves of diodes were analyzed for the calculation of the ideality factor n, density of the saturation current J_s and height of the potential barrier Φ_b. According to the diode theory of rectification, in thermionic-emission approximation the direct branch of I–V curve is described by the following expression [24,25]:

$$J = J_s\left(\exp\left[\frac{eU}{nkT}\right] - 1\right), \quad (2)$$

where k is Boltzmann's constant; T is absolute temperature of semiconductor. Ideality factor was $n = 1.61$ and was defined from the analysis of the linear portion of the direct branch of C–V curve using the following expression

$$\ln\frac{J}{J_s} = \frac{eU}{nkT}. \quad (3)$$

Extrapolation of $\ln(J/J_s)$ to the point $U = 0$ made it possible to establish the value $J_s = 1.29 \cdot 10^{-14}$ A/cm^2 based on the expression [23,24]:

$$J_s = A^*T^2\exp\left(-\frac{e\Phi_b}{nkT}\right), \quad (4)$$

where A^* — Richardson's constant. From the experimental data $A^* = 33.65$ A/(cm$^{-2} \cdot$ K^{-2}) at effective mass of electrons $m_n^* = 0.28m_0$, m_0 — electron mass in vacuum [1,2,6].

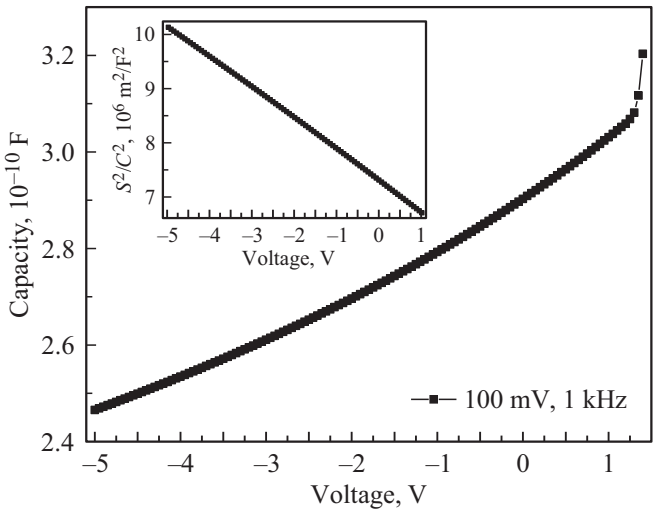


Figure 4. Capacitance voltage curve of SBD based on NiO/β-Ga_2O_3. The insert shows dependences of S^2/C^2 on voltage.

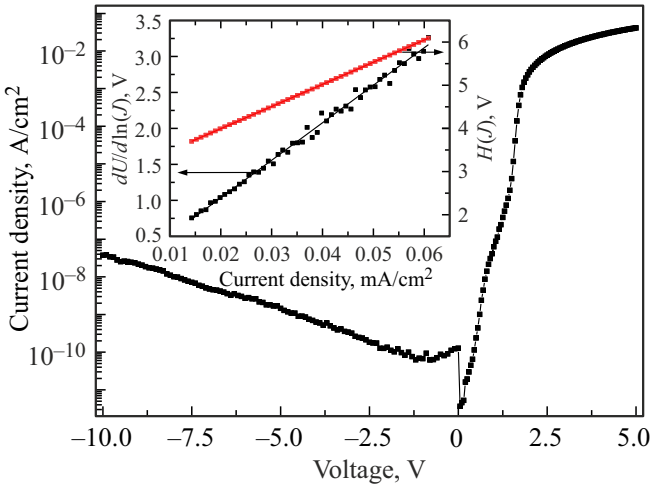


Figure 5. Current voltage curve of SBD based on NiO/β-Ga_2O_3. The insert shows curves of Cheung's method: $dU/d\ln(J)$ and $H(J)$ depending on J.

Based on the expression (4), the height of the potential barrier $\Phi_b = 1.63$ eV was calculated:

$$\Phi_b = \ln\left(\frac{A^*T^2}{J_s}\right)\left(\frac{nkT}{e}\right). \quad (5)$$

The C–V curve analysis was additionally conducted using Cheung's method [24,26]. The following ratios are true for SBD:

$$U = JR_sS + n\Phi_b + \frac{nkT}{e}\ln\left(\frac{J}{A^*T^2}\right), \quad (6)$$

$$H(J) = U - \frac{nkT}{e}\ln\left(\frac{J}{A^*T^2}\right), \quad (7)$$

where R_s is spreading resistance; S is anode surface area; H is function depending on J. Differentiation of

Electrical characteristics of Schottky diodes based on NiO/β-Ga_2O_3 structure

SBD parameters	Value	Method/note
Ideality factor n	1.61/1.58	TE-model/Cheung's method
Barrier height Φ_b, eV	1.63/1.62	TE-model/Cheung's method
Density of saturation current J_s, A/cm^2	$1.29 \cdot 10^{-14}$	TE-model
Rectification ratio at ± 2 V	$5.44 \cdot 10^7$	I–V curve
Breakdown voltage U_b, V	171	I–V curve
Breakdown field ε_b, MV/cm	3.55	–
Spreading resistance R_s, kOhm	1.22	Cheung's method
Contact potential difference U_k, V	1.29	C–V curve
Effective concentration $N_d - N_a$, cm^{-3}	$2.3 \cdot 10^{17}$	C–V curve

expression (7) with respect to J yields the following result:

$$\frac{dU}{d\ln(J)} = JR_sS + \frac{nkT}{e}. \quad (8)$$

From the analysis of dependence of $dU/d\ln(J)$ on J (see insert to Figure 5, black curve), $R_s = 1.22$ kOhm and $n = 1.58$ were defined. Based on expressions (7) and (8) it follows that

$$H(J) = JR_sS + n\Phi_b. \quad (9)$$

Dependence of $H(J)$ (see insert to Figure 5, red curve) makes it possible to establish $\Phi_b = 1.62$ eV using the previously obtained R_s and n. It should be noted that n and Φ_b, obtained using a thermionic emission (TE) model and Cheung's method differ slightly.

For the obtained Schottky diodes based on gallium oxide, C–V curves were studied in a wide range of reverse voltages with the purpose to establish the breakdown voltage. Breakdown voltage of diodes with an NiO layer was $U_b = 171$ V. For comparison, in diodes made previously without an NiO layer this value was equal to 131 V (Figure 6) [7]. The width of the spatial charge region (SCR) was assessed on the basis of the breakdown voltage value, effective concentration of the impurity defined from capacitance voltage curves (C–V curves) and the following expression:

$$d_{\text{scr}} = \sqrt{\frac{2\varepsilon_r\varepsilon_0(U_k + U)}{eN_d}}, \quad (10)$$

where d_{scr} is width of SCR, U_k is contact potential difference. The SCR width in breakdown voltage was ~ 940 nm, and the critical intensity of electric field ε_b — 3.55 MV/cm, which is rather close to the theoretical limit (8.2 MV/cm) for β-Ga_2O_3. The table presented main electric characteristics of SBD based on NiO/β-Ga_2O_3.

Figure 6 presents reverse current voltage curves of SBD based on NiO/β-Ga_2O_3 (black curve) and β-Ga_2O_3 (grey curve) [7]. C–V curves contain several specific regions corresponding to various mechanisms of leakage currents flowing.

For SBD based on NiO/β-Ga_2O_3 in the region of relatively low reverse voltages ($|U| \leq -45$ V) the dominant mechanism was thermionic field emission (TFE). This

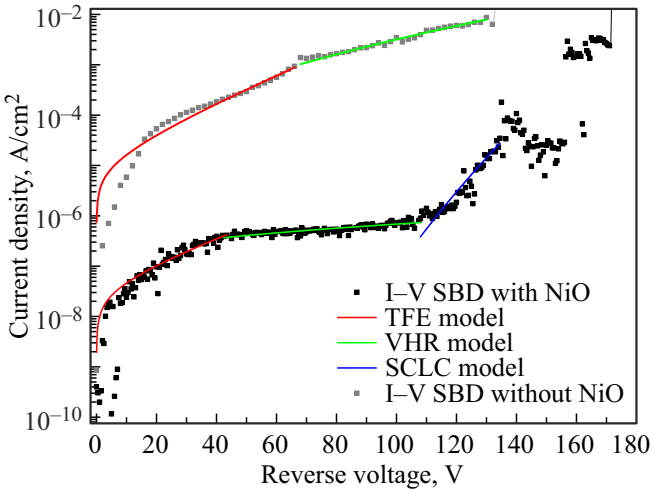


Figure 6. Reverse I–V curves of diodes based on NiO/β-Ga_2O_3 (black curve) and β-Ga_2O_3 (grey curve).

mechanism describes well the experimental data, since it accounts for both thermoelectronic emission above the potential barrier and tunneling of charge carriers through the barrier when exposed to electric current. The leakage current density within the TFE model is presented with the following expression:

$$J_{\text{tee}} = \frac{A^*Teh\varepsilon}{2k\pi}\sqrt{\frac{\pi}{2m^*kT}} \times \exp\left(-\frac{e}{kT}\left(\varphi_b - \Delta\varphi_{bl} - \frac{e(h\varepsilon)^2}{24m^*(2\pi kT)^2}\right)\right), \quad (11)$$

where J_{tee} is density of leakage current for the TFE-model, h is Planck constant, $\varepsilon = U/d_{\text{scr}}$ is electric field intensity, $\Delta]varphi_{bl}$ is lowering of barrier due to Schottky effect, $\text{cr}f(\varepsilon) = e(h\varepsilon)^2/24m^*(2\pi kT)^2$ is tunnel factor (the probability of tunneling through a triangular barrier [27,28]).

With further growth of voltage, a transition is observed towards the hopping transport with the variable range hopping (VRH) using Mott's model in the voltage range of -45 V $\leq |U| \leq -115$ V. Such conductivity mechanism is specific for wide-bandgap semiconductors with high density

of defects and interface states at a heterointerface. In the considered case for the NiO/β-Ga_2O_3 structure the reverse leakage current density is described with the following expression:

$$J_{\text{vrh}} = J_0\left(B\,\frac{e\varepsilon a}{2kT}\left(\frac{T_0}{T}\right)^{0.25}\right), \qquad (12)$$

where J_{vrh} is density of leakage current for the VRH-model, T_0 is characteristic Mott's temperature, a is radius of localization, B is constant [16]. VRH is the main mechanism of leakage current in this SBD, since it prevails in a wide interval of voltages (from -45 to -115 V).

In the field of high reverse voltages ($|U| > -115$ V) the conductivity depends on the currents limited by a space charge (space-charge limited current, SCLC). The experimental dependence of current on voltage follows the power law $I \sim U^b$ [28]. The power exponent b rises to 6, which is due to the presence of high concentration of traps in the band gap β-Ga_2O_3.

5. Conclusion

The paper presents the results of the study of vertical diodes with Schottky barrier based on β-Ga_2O_3 with a solid NiO layer formed by the method of magnetron sputtering. The produced SBDs demonstrated high values of rectification coefficient $5.44 \cdot 10^7$ and breakdown voltage 171 V, which corresponds to electric field intensity of 3.55 MV/cm.

The use of the solid NiO layer made it possible to reduce the density of the reverse leakage current by 2–3 orders of magnitude compared to the classic SBDs by formation of a heterobarrier and partial suppression of the edge effect.

The complex analysis of the reverse branch of current voltage curve at room temperature showed serial change of leakage current mechanisms: in the area of low voltages $U \leq 45$ V the leakage current is defined by thermionic field emission; in the interval of voltages of $45\,\text{V} < U \leq 115\,\text{V}$ the conductivity of the structure depends on the hopping transport using the Mott's model; at voltages of $U > 115$ V the conductivity prevails that depends on currents limited by space charge.

Funding

The results of the study were obtained within the state assignment of the Ministry of Education and Science of Russia, project No. FSWM-2025-0021.

Conflict of interest

The authors state that they have no conflict of interest.

References

[1] K. Zeng, A. Vaydai, U. Singisetti. IEEE Electron Dev. Lett., **39**, 1385 (2018). DOI: 10.1109/LED.2018.2859049.

[2] M. Orita, H. Ohta, M. Hirano, H. Hosono. Appl. Phys. Lett., **77**, 4166 (2000).

[3] H. He, R. Orland, M.A. Blanco, R. Pandey, E. Amzallag, I. Baraille, M. Rérat. Phys. Rev. B, **74**, 195123 (2006).

[4] Y. Liu, S. Roy, C. Peterson, A. Bhattacharyya, S. Krishnamoorthy. AIP Advances, **15**, 015114 (2025). https://doi.org/10.1063/5.0251069

[5] T. Onuma, S. Saito, K. Sasaki, T. Masui, T. Yamaguchi, T. Honda, M. Higashiwaki. Jpn. J. Appl. Phys., **54**, 112601 (2015).

[6] A. Almaev, N. Yakovlev, A. Tsymbalov, V. Kopyev, P. Butenko, M. Boiko, V. Krymov, B. Kushnarev, S. Shapenkov, M. Sharkov, A. Zarichny. J. Vac. Sci. Technol. A, **42** (8), 042802 (2024). DOI: 10.1116/6.0003618

[7] N.N. Yakovlev, A.V. Almaev, B.O. Kushnarev, M.G. Verkholetov, M.V. Poliakov, M.M. Zinovev. Crystals, **14** (2), 123 (2024). DOI: 10.3390/cryst14020123

[8] V.V. Kopyev, N.N. Yakovlev, A.V. Tsymbalov, D.A. Almaev and P.V. Kosmachev. Micromachines, **17** (1), 100 (2026). https://doi.org/10.3390/mi17010100

[9] J. Wan, H. Wang, C. Zhang, Y. Li, C. Wang, H. Cheng, J. Li, N. Ren, Q. Guo, K. Sheng. Appl. Phys. Lett., **124**, 24 (2024). https://doi.org/10.1063/5.0211183

[10] H. Sheoran, V. Kumar, R. Singh. ACS Appl. Electron. Mater., **4**, 6 (2022). DOI: 10.1021/acsaelm.2c00101

[11] B. Fu, Z. Jia, W. Mu, Y. Yin, J. Zhang, X. Tao. J. Semicond., **40**, 011804 (2019). DOI: 10.1088/1674-4926/40/1/011804

[12] S.E. Bennett. Mater. Sci. Technol., 26, 9 (2010). DOI 10.1179/026708310X12668415533685

[13] S. Kitagawa, H. Miyake, K. Hiramatsu. Jpn. J. Appl. Phys., **1** (53), 05FL03 (2014).

[14] T. Igarashi, Y. Ueda, K. Koshi, R. Sakaguchi, S. Watanabe, S. Yamakoshi, A. Kuramata. Phys. Status Solidi B, **262**, 2400444 (2025).

[15] M. Higashiwaki. IEEE Electron Dev. Mag., **2**, 42–C3 (2024).

[16] M. Xiao, B. Wang, J. Spencer, Y. Qin, M. Porter, Y. Ma, Y. Wang, K. Sasaki, M. Tadjer, Y. Zhang. Appl. Phys. Lett., **122**, 183501 (2023). https://doi.org/10.1063/5.0142229

[17] A.S. Nair, S. Nair, L.R. Thoutam. Materials Today Electron., **57**, 101824 (2025). https://doi.org/10.1016/j.mtelec.2025.101824

[18] M. Labed, J.H. Park, A. Meftah, N. Sengouga, J.Y. Hong, Y.-K. Jung, Y.S. Rim. ACS Appl. Electron. Mater., **3**, 3667 (2021). https://doi.org/10.1021/acsaelm.1c00647

[19] X. Lu, Y. Deng, Y. Pei, Z. Chen, G. Wang. J. Semicond., **44**, 061802 (2023). https://doi.org/10.1088/1674-4926/44/6/061802

[20] Z. Zhang, Q. Song, D. Liu, Y. Yan, H. Chen, C. Mu, D. Chen, Q. Feng, J. Zhang, Y. Zhang, Y. Hao, C. Zhang. Sci. China Mater., **67** (5), 1646 (2024). https://doi.org/10.1007/s40843-023-2801-2

[21] W. Hao, F. Wu, W. Li, G. Xu, X. Xie, K. Zhou, X. Zhou, Q. He, X. Zhao, S. Yang. IEEE Trans. Electron Dev., **70** (4), 2129 (2023). https://doi.org/10.1109/TED.2023.3241885

[22] Y. Liu, S. Roy, C. Peterson, A. Bhattacharyya, S. Krishnamoorthy. AIP Adv., **15**, 015114 (2025). https://doi.org/10.1063/5.0251069

[23] M. Xiao, B. Wang, R. Zhang, Q. Song, J. Spencer, Z. Du, Y. Qin, K. Sasaki, H. Wang, M. Tadjer, Y. Zhang. *35th Int. Symp. on Power Semiconductor Devices and ICs* (ISPSD 2023), 29 May–1 June, 2023, Hong Kong, China. https://doi.org/10.1109/ISPSD57135.2023.10147704

[24] H. Sheoran, V. Kumar, R. Singh. ACS Appl. Electron. Mater., **4**, 2589 (2022). https://doi.org/10.1021/acsaelm.2c00101
[25] Y. Yao, R. Gangireddy, J. Kim, K.K. Das, R.F. Davis, L.M. Porter. J. Vac. Sci. Technol. B, **35**, 03D113 (2017). https://doi.org/10.1116/1.4980042
[26] S.K. Cheung, N.W. Cheung. Appl. Phys. Lett., **49**, 85 (1986). https://doi.org/10.1063/1.97359
[27] X. Xia, M. Xian, P. Carey, C. Fares, F. Ren, M. Tadjer, S.J. Pearton, T.Q. Tu, K. Goto, A. Kuramata. J. Phys. D: Appl. Phys., **54** (30), 305103 (2021). https://doi.org/10.1088/1361-6463/abfe37
[28] B. Wang, M. Xiao, X. Yan, H.Y. Wong, J. Ma, K. Sasaki, H. Wang, Y. Zhang. Appl. Phys. Lett., **115**, 263503 (2019). https://doi.org/10.1063/1.5132818

Translated by D.Safin